

# MOBILITY CHARACTERIZATION OF P-TYPE AND N-TYPE STRAINED $\text{Si}_{1-x-y}\text{Ge}_x\text{C}_y/\text{Si}$ EPILAYER HALL DEVICES

Jeff J. Peterson<sup>1</sup>, Charles E. Hunt<sup>1</sup>, Stefan F. Zappe<sup>2</sup>, Ernst Obermeier<sup>2</sup>, Richard Westhoff<sup>3</sup>, McDonald Robinson<sup>3</sup>

<sup>1</sup> Department of Electrical and Computer Engineering; University of California, Davis; Davis, CA 95616

<sup>2</sup> Microsensor and Actuator Technology; Technical University of Berlin; D-13355 Berlin, Germany

<sup>3</sup> Lawrence Semiconductor Research Laboratory, Inc.; Tempe, AZ 85282

## ABSTRACT

Mobilities in  $\text{Si}_{1-x-y}\text{Ge}_x\text{C}_y$  layers were measured using mesa etched Van der Pauw structures for alloy layers with  $0 < x < 0.30$  and  $0 < y < 0.02$  and doping levels of  $10^{15} < N < 10^{18} \text{ cm}^{-3}$ . Mobilities in  $\text{Si}_{1-x-y}\text{Ge}_x\text{C}_y$  layers with  $x = 0.27$  were found to approach Si mobilities for both  $\mu_n$  and  $\mu_p$ . While electron mobilities in phosphorous-doped SiGeC decrease with doping concentration, hole mobilities in boron-doped SiGeC increase with doping level, indicating ionized impurity scattering is not dominant for  $\mu_p$  over the temperature range studied.

## INTRODUCTION

As advantages of SiGeC alloys become clear, it is critical to understand the effect of substitutional and interstitial C incorporation on mobility and other carrier properties. The purpose of this work is to address the effect that C incorporation into SiGe has on carrier mobilities. To our knowledge, this is the first time this subject has been addressed in a systematic manner for this material system in the literature.

## EXPERIMENT

Strained  $\text{Si}_{1-x-y}\text{Ge}_x\text{C}_y$  epitaxial layers on (100) Si were grown using atmospheric-pressure chemical vapor deposition (APCVD) at temperatures ranging from 625°C to 675°C. Ge compositions of these epilayers range from  $x = 0$  to  $x = 0.30$  and C compositions from  $y = 0$  to  $y = 0.02$  as determined using Rutherford back-scattering (RBS) analysis. Analysis of similar layers using double crystal x-ray diffraction (DCXRD) has shown this material to be fully strained with compressive strain occurring in the plane parallel to the heterojunction and tensile strain along the axis normal to the heterojunction. It should be pointed out that the C concentrations found by RBS include both substitutional and interstitial C atoms. Raman and FTIR measurements on similar samples (unpublished, performed in collaboration with the University of Barcelona) has shown the ratio of substitutional C to interstitial C to decrease as the total C concentration in the alloy layer is increased. For low C concentrations (~1%), most of the C incorporation occurs substitutionally. The layers in this present study have not been measured using these methods, but from previous measurements we would estimate the C to be incorporated substitutionally for the greatest part. Epilayer thickness, ranging from 191nm to

348nm, was also determined by RBS and verified using spreading resistance profiling (SRP). Epitaxial doping levels were determined using SRP to range from  $10^{15}$  to  $10^{18}$  cm<sup>-3</sup>.

Hall measurement structures were formed by mesa-etching Si<sub>1-x-y</sub>Ge<sub>x</sub>C<sub>y</sub> epitaxial layers to define discrete Van der Pauw or 'Greek cross' structures extending completely through each epilayer; Figure 1(a) shows a plan view of the 1mm Van der Pauw structure used for the measurements in the present work.

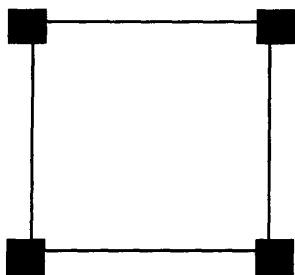


Figure 1(a) - Plan view of the 1mm x 1mm Van der Pauw structure used for Hall measurements.

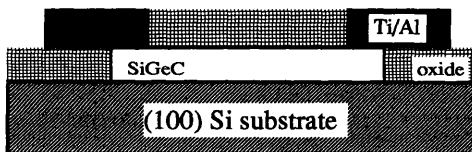


Figure 1(b) - Cross-section of the Hall measurement structure.

These patterns were mesa-etched through the strained SiGeC epilayers using either reactive ion etching (RIE) or standard wet etching. RIE etching was done using an SF<sub>6</sub>/O<sub>2</sub> gas mixture at 7.5sccm and 2.5sccm, respectively, and a pressure of 100mTorr. Wet mesa-etch samples were formed using HNA etching at room temperature. After mesa-etch, all samples were examined using a standard differential step-height profilometer to verify that the Hall structures extend completely through each epilayer. The Hall structures were next covered by an oxide dielectric layer, patterned for contact holes, and covered by Ti/Al metallization deposited using electron-beam evaporation. A final patterning step on the Ti/Al layers followed by a standard clean step and a 425°C/30 minute furnace anneal in forming gas, results in contact to the measurement structures via bondpads. Finally, the backside oxide was removed and the wafer cleaned. Figure 1(b) shows a cross-section of the completed measurement structure; note that this structure is measuring the in-plane mobility. After fabrication, samples were diced using a wafer saw and placed into dual in-line packages (DIP) for measurement.

Hall measurements were performed using the Keithley model 7065 Hall Measurement system, over a temperature range of 83K to 673K with a magnetic field strength of 4.8KG. The Hall coefficient for this setup is estimated to be 1.18 assuming lattice scattering dominates these measurements [1].

## RESULTS/DISCUSSION

Figure 2 shows a plot of hole mobilities in boron-doped SiGeC layers on p-type (100) Si. Measurement results for four strained SiGeC/Si samples, as well as for a reference Si device constructed simultaneously with these samples, are represented by the symbols enclosed by the legend box in Figure 2. Also shown are reference curves for hole mobilities in unstrained Si from Jacoboni et al. [2] and for hole mobilities in strained SiGe channels from Wang et al. [3].

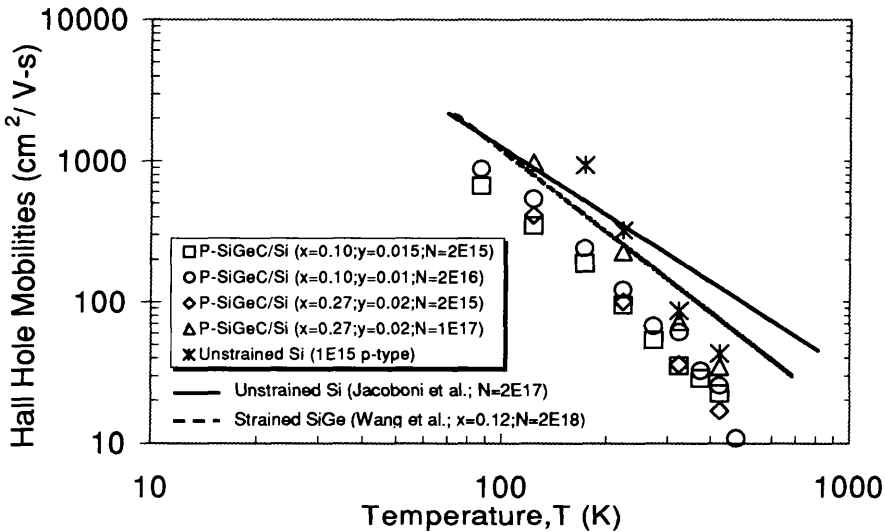


Figure 2 – Measured hole mobilities ( $\mu_p$ ) in boron-doped SiGeC layers on p-type Si (composition and doping shown in legend) and a single unstrained Si substrate. The lines represent reference data from the literature. Solid line: unstrained Si  $\mu_p$  from Jacoboni et al. [2]. Dashed line:  $\mu_p$  in strained SiGe channels from Wang et al. [3].

Figure 2 shows the strained SiGeC hole mobilities to be slightly below those for the Si reference device. In comparing the slope of the mobility vs. temperature, both reference Si and strained SiGeC layer curves have slightly higher slopes than the curves from literature, which we have not explained at this time. At a temperature of 123 K, the alloy layer combining high Ge concentration ( $x = 0.27$ ) and high doping ( $N_A = 1 \times 10^{17} \text{ cm}^{-3}$ ) has the highest SiGeC  $\mu_p$  value we measured in this work,  $900 \text{ cm}^2/\text{V-s}$ ; this exceeds the  $\mu_p$  for Si data from the literature [2]. In comparing data series 1 to 3 and data series 2 to 4, it is seen that the layers with higher Ge concentrations have enhanced mobilities over those that have lower Ge concentrations when other parameters are equal.

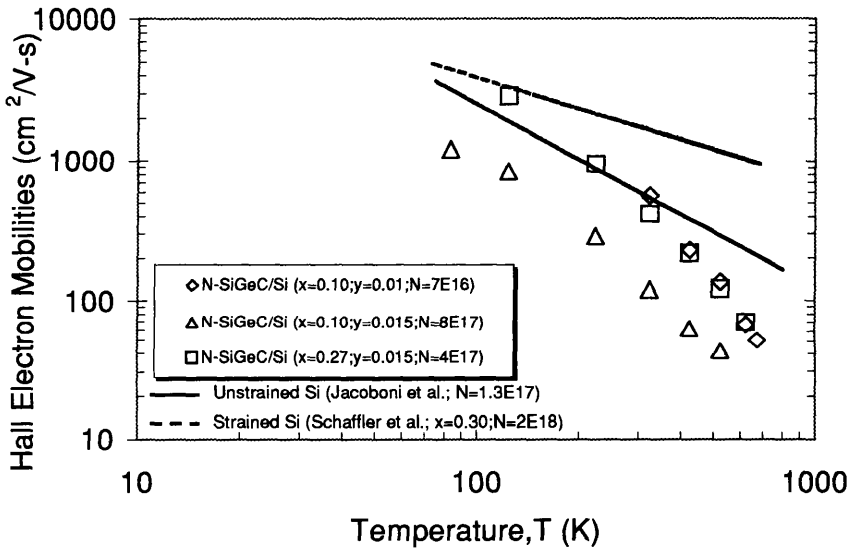


Figure 3 – Measured electron mobilities ( $\mu_n$ ) in phosphorous-doped SiGeC layers on n-type Si (composition and doping shown in legend). The lines represent reference data from the literature. Solid line: unstrained Si  $\mu_n$  from Jacoboni et al. [2]. Dashed line:  $\mu_n$  in strained Si on SiGe from Schaffler et al. [4].

Figure 3 shows a plot of electron mobilities for phosphorous-doped SiGeC layers on n-type (100) Si. Measurement results for three strained SiGeC/Si samples are represented by the symbols enclosed in the legend box; also shown in Figure 3 are reference curves for electron mobilities in unstrained Si from Jacoboni et al. [2] and for electron mobilities in strained Si on SiGe taken from Schaffler et al. [4]. Similar to the results seen for hole mobilities,  $\mu_n$  is enhanced for alloy layers with increased Ge concentrations; this may be seen in Figure 3 by comparing curves 2 and 3. Figure 3 also shows two alloy layers with  $\mu_n$  that exceeds that found in the literature for Si (shown by the solid line). At a temperature of 123 K, we measured the highest  $\mu_n$  recorded for strained SiGeC layers in this work with a value of  $2880\text{cm}^2/\text{V-s}$  ( $x = 0.27, y = 0.015, N_d = 4 \times 10^{17}\text{cm}^{-3}$ ). It is expected that the  $\mu_n$  for the alloy layer in the first data series in Figure 3 ( $x = 0.10, y = 0.01, N_d = 7 \times 10^{16}\text{cm}^{-3}$ ) will display even higher mobilities when the measurements are extended to lower temperatures.

An examination of the  $\mu_n$  versus temperature slope in Figure 3 shows that an inflection point in the slope occurs at about 200 K. We believe this to be the temperature at which ionized impurity scattering dominates the  $\mu_n$  of the alloy layer. Figure 2 shows that this effect is not present in the  $\mu_p$  versus  $T$  curves.

Figure 4 shows the effect of alloy doping levels on SiGeC mobilities for temperatures of 323 K. Also shown are reference curves from Jacoboni et al. for both n-type (solid line) and p-type (dashed line) unstrained Si layers [2].

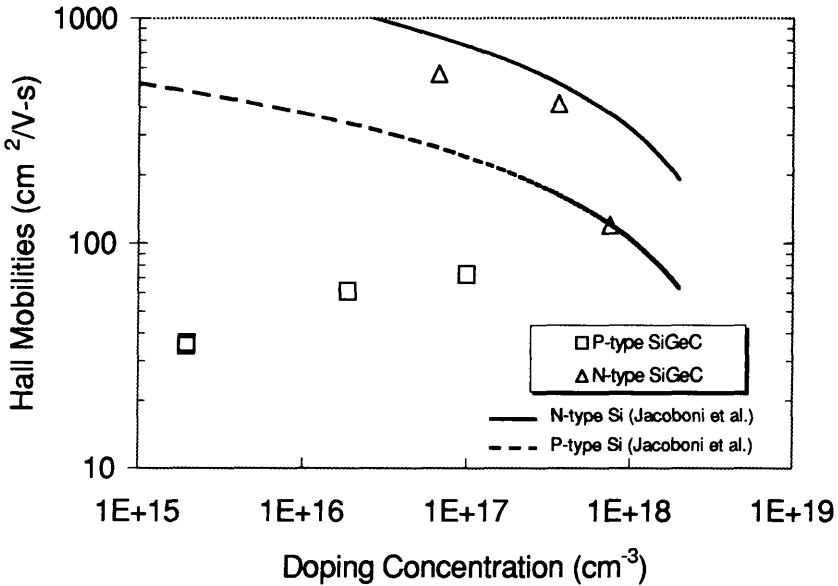


Figure 4 - Measured doping effect on strained SiGeC mobilities at 323 K. The lines show 300K reference data from Jacoboni et al.[2]. Solid line: unstrained n-type Si. Dashed line: unstrained p-type Si.

Figure 4 shows that the behavior of SiGeC  $\mu_n$  parallels the unstrained Si reference quite well, indicating that ionized impurity scattering appears to affect the SiGeC  $\mu_n$  in a way quite similar to Si. The effect of doping on the SiGeC  $\mu_p$  is quite different from the doping effect on Si, however; our data shows that the SiGeC  $\mu_p$  increases with doping level, suggesting that  $\mu_p$  is not dominated by ionized impurity scattering. While these data indicate that the limiter for  $\mu_p$  in SiGeC layers is a mechanism other than ionized impurity scattering, we do not know from these measurements that ionized impurity scattering is not occurring at a rate comparable to that in Si – only that any ionized impurity scattering which may be present is not the dominant scattering mechanism at this temperature.

We propose a theory to account for the rise in SiGeC  $\mu_p$  with doping, which is shown in Figure 4. We suggest that the effect could be explained by boron induced strain in the alloy layers. The incorporation of boron in SiGe layers has previously been shown to introduce strain into the alloy layer. The  $\mu_p$  in SiGe has also been shown in previous work to increase with both

tensile and compressive stress [5]. We propose that increased boron incorporation in these p-type SiGeC layers is resulting in  $\mu_p$  enhancement by increasing strain in the alloy layer.

Measurements on anisotype SiGeC/Si structures have also been initiated. In isotype n-type SiGeC/n-type Si heterojunctions, the possibility exists for small amounts of parallel conduction (in the substrate) leading to a slight over-estimate of the mobility. While the valence band discontinuity makes parallel conduction for p-type SiGeC/p-type Si unlikely, n-type mobility measurements may be refined to account for parallel conduction of the order of several percent.

## CONCLUSIONS

We have studied the electron and hole mobilities in strained  $\text{Si}_{1-x}\text{Ge}_x\text{C}_y$  layers using Hall effect mobility measurements. Carrier mobilities in these layers were found to increase with increasing Ge concentration; for  $x = 0.27$ , SiGeC  $\mu_n$  and  $\mu_p$  approach or exceed carrier mobilities for unstrained Si. While electron mobilities in SiGeC decrease with doping concentration, hole mobilities rise indicating ionized impurity scattering is not the limiting factor for  $\mu_p$  over the temperature range studied. Work is underway to explore this effect over a wider range of dopant concentrations.

## ACKNOWLEDGEMENTS

This project was supported by Lawrence Semiconductor Research Laboratories, Inc., UC MICRO, ONR#N00014-93-C-0114, and ONR#N00014-96-C-0219. Devices were fabricated in the UC Davis Microfabrication Facility.

## REFERENCES

1. D. K. Schroder, *Semiconductor and Device Characterization*, John Wiley & Sons, Inc., New York, 1990, p. 199.
2. C. Jacoboni, C. Canali, G. Ottaviani, and A. Quaranta, *Solid-State Electronics* **20**, pp. 77-89 (1977).
3. P.J. Wang, B.S. Meyerson, F.F. Fang, J. Nocera, and B. Parker, *Appl. Phys. Lett.* **55**, pp. 2333-2335 (27 November 1989).
4. F. Schaffler, D. Tobben, H-J Herzog, G. Abstreiter, and B. Hollander, *Semicond. Sci. Technol.* **7**, pp. 260-266 (1992).
5. S. C. Jain, *Germanium-Silicon Strained Layers and Heterostructures*, Academic Press, San Diego, 1994, p. 90.